ANALYSIS OF THE DYNAMICS OF CDMA REVERSE LINK POWER CONTROL

Kenji Leibnitz*, Phuoc Tran-Gia*, and John E. Miller**

* *University of Würzburg, Institute of Computer Science, Am Hubland, 97074 Würzburg, Germany*
{leibnitz|trangia}@informatik.uni-wuerzburg.de

** *NORTEL Wireless Networks, 2201 Lakeside Blvd., Richardson, TX 75082-4399, USA*
millerj@nortel.com

In this paper we develop an analytical expression for the mobile station transmit power based on a discrete time and state space. In our model we focus on the time-varying distortions found in a CDMA reverse link channel, network delays, and the fluctuations in multi-access interference. Based on this description we are able to characterize the dynamic behavior of the power control loop and its reaction time to batch arrivals and departures. We also give an expression for exceeding the dynamic range of the discrete-step power control algorithm, allowing a systems engineer to calculate the trade-offs between capacity and coverage of the system.

1 INTRODUCTION

Code division multiple access (CDMA) is the upcoming standard RF access technology for third generation mobile communication systems. Its greatest advantage over conventional systems lies in the increase in capacity due to the application of spread spectrum technology. By spreading the transmitted signal over a larger bandwidth, the harmful effects of interference from other users can be mitigated. This robustness towards interference must be compensated at the cost of keeping the received signal strength from each mobile station (MS) at the base transceiver station (BTS) at equal levels. This, however, requires that the CDMA system overcomes the so-called "near-far" problem, where signals from users that are close to the BTS are much stronger and therefore eliminate the signals of other users located at greater distances.

To solve this problem, transmit *power control* in the reverse link (mobile-to-base station path) of mobile systems based on direct sequence spread spectrum for code division multiple access (DS-CDMA) is performed. The air interface standard IS-95A [10] carefully specifies a reverse link power control algorithm and its accompanying parameters. The performance of this *signal-to-interference-ratio* (SIR) balancing algorithm based on local SIR estimates has been studied by many authors. Viterbi [13] constructed an analytical model containing inner loop processing (based on SIR) and outer loop processing based on frame error performance. Ariyavisitakul et al. [1] conducted a simulation study of single and multi-cell systems and examined the dependence of signal and interference statistics on step size and processing delays. The effects of power control non-idealities on performance were investigated [2] and [7]. Distributed algorithms which use network-wide information have also been examined, see [3] and [5].

The goal of this work is to formulate a comprehensive analytical model for the power control loop in [1]. The motivation behind this goal is to find a robust model of reverse link power control which will clearly illustrate the trade-offs between system parameters and their impact on performance. System parameters include step size, processing delay, traffic loading, loop dynamic range, and path loss. The model we propose is a Markov state space representation of the portion of the mobile transmit power controlled by the inner power control loop. This model follows naturally from the IS-95A specification since it specifies a power control step size as well as an inner loop dynamic range. These conditions result in a quantization of the reverse-link inner loop transmit power "states" that the mobile may occupy. This approach allows direct computation of the statistics of the portion of the mobile transmit power controlled by the inner loop and it results in a convenient computational model which clearly shows the effect of the system parameters on the inner loop processing. The model may be used to compute the time-dependent loop response or to compute the probability of exceeding the mobile's inner loop dynamic range which can have serious implications on outage, coverage and capacity.

The remainder of this paper is organized as follows. Section 2 gives an overview of the power control model and the basic relations involved in the loop. In Section 3 we derive our analytical Markov chain model and its implications on the dynamics of the system. The results of these effects are given in Section 4 and it is followed by the conclusion and outlook on future work in Section 5.

2 POWER CONTROL MODELING AND BASIC RELATIONS

This section describes the basic relations involved in the inner loop reverse link power control algorithm. In the following, we will be considering the model of the loop presented in [1], see Fig. 1.

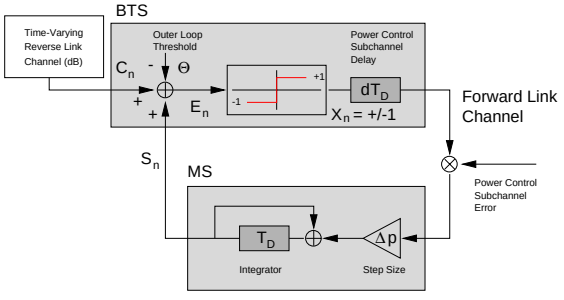

Figure 1: Model for the inner loop

The main goal of the power control algorithm is to over-

come the "near-far" problem, i.e., to keep the received power of all mobiles at the base station (nearly) equal and to track time-varying channel loss. This is achieved by the close inter-working of two power control loops, the inner and outer loop. The outer loop evaluates the current frame error rate and adjusts the target SIR threshold accordingly. In the inner loop, the base station compares the received signal level of each mobile with the outer loop threshold in order to track the desired signal-to-interference ratio. If the mobile power is too low, the base station will transmit a "power up" command bit on the power control sub-channel of the forward link. Consequently, a too high power level will result in the transmission of a "power down". It is not possible for the mobile to maintain its current signal level.

The command bit is sent without error-coding, thus resulting in a higher error probability than for the other data transmitted on the forward link. It has been shown, however, that under certain conditions, power control bit errors can have little impact on performance [1], [12].

Upon reception of the power control bit the mobile will update its transmit power by a fixed step size, predefined here to 1 dB. This update is performed every power control cycle (defined here as a time interval of 1.25 ms). The processing of the power control command requires a sub-channel delay of 3 cycles causing that a power control update computed at time n will take effect at cycle $n+3$.

3 ANALYTICAL MODEL OF THE POWER CONTROL LOOP

In our analytical model we will focus on the time dynamics of the mobile transmit power. Since both, the time increments and the power updates are discrete values of 1.25 ms and 1 dB, respectively, we can model the transmit power in a discrete time and state space. In the IS-95 system the range for the MS transmit power is between -50 dBmW and 23 dBmW. In the following, we will use an abstract indexing of power levels, i.e., $j = 0, \ldots, J$ with J total power levels. This generalized notation will facilitate any further work considering different power update step sizes.

Let S_n be a random variable representing the mobile transmit power at power control cycle n. We will then refer to the probability that the mobile is transmitting during n at power level j as $s_n(j)$.

The transmission over the reverse link channel attenuates the signal that the mobile originally sent by the *channel loss*. This loss is modeled here by the random variable C_n. The base station compares the received signal with the outer loop threshold θ and determines the power control command. We model this command as the random variable X_n and define the probability for stepping up from level j as $u_n(j)$. Consequently, the probability for a "power down" command is given by $d_n(j) = 1 - u_n(j)$. Please, note that the index n indicates the time of computation of the power control command prior to the sub-channel delay.

3.1 Model Parameters

As mentioned in Section 2 the aim of the reverse link power control is to provide compensation for time-varying channel losses and eliminate near-far induced multi-access interference. This may be modeled by a control loop which forces the effective symbol energy to noise spectral density ratio $(E_s/N_0)_{\text{eff}}$ to some threshold. This section presents a system-level model for the $(E_s/N_0)_{\text{eff}}$ which includes such parameters as the subscriber population and the maximum number of active users allowed in the system. While some researchers have found that normal fluctuations in subscriber traffic have little effect on power control performance [1], we wish to include it here so that we may account for the effects of batch arrivals and departures.

We may define a quantity which we will refer to as the *loading factor* $F = \frac{I}{I+N}$ where I is the total interference power and N is the noise power. Similar quantities have been defined by other authors [6]. It is easy to show that the signal-to-interference-and-noise-ratio (SINR) is related to F by the expression: SINR $= \frac{\tilde{S}}{I+N} = \frac{\tilde{S}}{N} \cdot (1-F)$ where $\tilde{S}$ is the received signal power. If the system supports only a single user, the loading is zero and the SINR $=$ SNR, if the loading is maximum $I \gg N$, the loading is unity and the SINR is zero.

We may derive a more direct relationship between the number of active users and the average interference. Consider that the interference power is some fraction of the interference and noise power $I = \varepsilon(I+N) = \varepsilon(k_p - 1)\tilde{S}$ where $0 \leq \varepsilon \leq 1$, $\tilde{S}$ is the power of each interfering signal (they are all assumed to be equal), k is the number of active users and k_p is defined as the maximum number of active users supported by an interference-limited system. This *pole capacity* is approximately $k_p \approx (W/R)/(E_s/N_0)_{\text{eff}} + 1$ with the spreading bandwidth W and data bitrate R. Using these relationships we can see that $F = \varepsilon = (k-1)/(k_p - 1)$. If we consider that $E_s \approx \tilde{S}/R$ and $I_0 + N_0 \approx I/W + N/W$, a convenient relationship for $(E_s/N_0)_{\text{eff}}$ results:

$$\left(\frac{E_s}{N_0}\right)_{\text{eff}} = \frac{E_s}{I_0 + N_0} = \frac{W}{R} \cdot \frac{\tilde{S}}{N} \cdot \left(\frac{k_p - k}{k_p - 1}\right) \qquad (1)$$

So, fluctuations in the subscriber population result in a linear fluctuation in the $(E_s/N_0)_{\text{eff}}$. The quantity in parentheses represents an interference-induced loss. If k_p is large, then the arrival or departure of a few users will be negligible. However, if a batch arrival or departure occurs the fluctuation in $(E_s/N_0)_{\text{eff}}$ could be substantial. The effect of these traffic-induced fluctuations on control-loop dynamics is of particular interest here.

3.2 Gaussian Channel Model

A mobile transmits a signal to the base station at power level S_n. While traversing the reverse link channel it is being attenuated due to propagation loss, multi-path effects, and shadow fading. We can therefore define the received

signal at the base station (in dB) $\tilde{S} = S + (L + Z)$ as sum of the transmitted signal and the channel loss, which contains the propagation loss L and the loss due to shadow fading Z. For our model we will use the well known Hata model [8] for computing L and shadowing will be described by a zero mean Gaussian random variable.

We can then rewrite Eqn. (1) for a given user at power control cycle n like in Eqn. (2). Please note that from now on all quantities given here are in dB:

$$\left(\frac{E_s}{N_0}\right)_{\text{eff,dB}} = \left(\frac{W}{R}\right)_{\text{dB}} + (S_{n,\text{dB}} + L_{n,\text{dB}} + Z_{n,\text{dB}}) - N_{\text{dB}} + \left(\frac{k_p - k}{k_p - 1}\right)_{\text{dB}} \quad (2)$$

As a first step we will include all factors except for S_n in our loop driving variable of the channel loss C_n which we will model as i.i.d. Gaussian random variable with mean $\mu_C = \frac{W}{R} + L_n + E[Z_n] - N + \frac{k_p - k}{k_p - 1}$ and standard deviation σ_C. For the other random variable Z_n, we need to observe the mean value, indicated by $E[\cdot]$.

The probability for a "power up" command at cycle n can then be computed by comparing the $(E_s/N_0)_{\text{eff}}$ value with the threshold θ obtained from the outer loop. For the sake of simplicity we will assume here a fixed value of θ = 14 dB.

$$P(\text{"power up"}) = P\left(\left(\frac{E_s}{N_0}\right)_n \leq \theta\right)$$

This leads us to the probability for "power up" from a power level j as:

$$u_n(j) = \frac{1}{2} + \frac{1}{2} \cdot \text{erf}\left(\frac{\theta - j - \mu_C}{\sqrt{2} \cdot \sigma_C}\right)$$

Since we currently have not included any time-dependent behavior of the channel, we can also drop the time index n and simply write $u(j)$. The probabilities $u(j)$ for a "power up" command depending on the mobile transmit power j are depicted in Fig. 2. Increasing the number of users in the cell results in a worse $(E_s/N_0)_{\text{eff}}$ ratio (via the multi-access interference term) and therefore the probability of "power up" for power levels below the desired threshold increases as well.

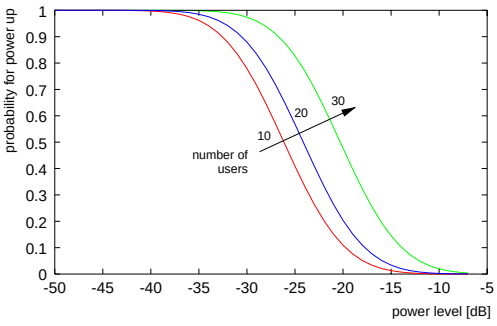

Figure 2: Probabilities for "power up" command

3.2.1 Dependency Structure and Markov Chain Description

The time dependent behavior of the inner loop can be greatly influenced by the power control sub-channel delay which causes the power control command to take effect 3 time increments after the up/down command was issued. The three step delay results from a $d = 2$ step delay in Fig. 1 and an additional delay of one time increment due to mobile processing delays.

Transitions from one discrete power level to the next take place each cycle and are only performed between adjacent levels. The dependency structure of the power levels for reaching a given level j is illustrated in Fig. 3(a).

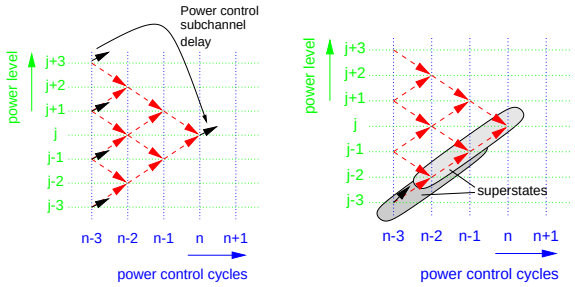

(a) Dependencies of power levels

(b) Super-state transitions

Figure 3: Power control model state transitions

Fig. 3(a) illustrates that the power control command "up" for level j at time n depends on the probabilities for "power up" of the 4 possible states that could have been assumed 3 cycles before, i.e., levels $j + 3$, $j + 1$, $j - 1$, and $j - 3$ at time $n - 3$. Note that for state j it is not possible to have been in the same state 3 cycles before.

Since the probability for each state at time $n - 3$ is computed by an equivalent subtree structure, we are also dependent on the probability of reaching these originating states at time $n - 3$. We therefore cannot simply assume that the probabilities $u_n(i)$ are the transition probabilities in our case because we must also include the paths for reaching these states. In order to incorporate these paths as well, we define new super-states $\bar{s}_n(j_1, j_2, j_3)$ containing 3 successive ordinary states which indicate the sequence that was taken.

$$\bar{s}_n(j_1, j_2, j_3) = P(S_n = j_3 | S_{n-1} = j_2, S_{n-2} = j_1)$$

Since we only have transitions between neighboring states to $j_2 = j_1 \pm 1$ and $j_3 = j_2 \pm 1$, we can further limit the state space. In this case we have $4(J + 1)$ possible preceding super-states $\bar{s}_{n-1}(j_1, j_2, j_3)$ and a transition to super-state $\bar{s}_n(j_2, j_3, j_4)$ takes place with $u_{n-3}(j_1)$ or $d_{n-3}(j_1)$ depending on whether $j_4 = j_3 + 1$ or $j_4 = j_3 - 1$. The transitions between super-states will then look like in Fig. 3(b).

Based on these super-state transitions, it is possible to give a state space diagram at time n with the transition probabilities given by $u_n(i)$ and $d_n(i)$, see Fig. 4.

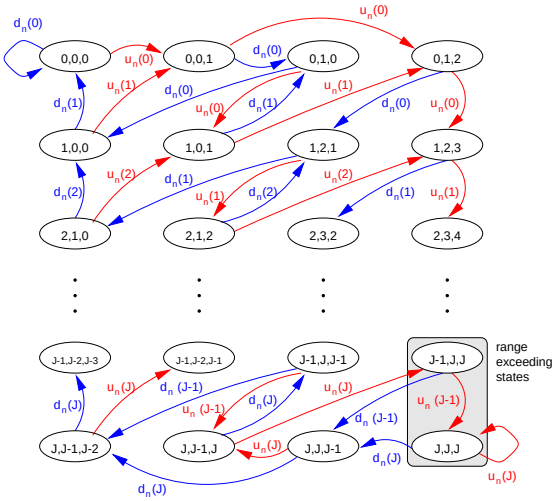

Figure 4: Super-state space of Markov chain

The transition probabilities at time n can be ordered in a Matrix $\mathcal{P}_n$.

3.3 Non-Stationary Case

We first consider a non-stationary case, where we start off with an initial mobile transmit power distribution S_0 at time $n = 0$ and iteratively compute the successive power distribution S_n of the considered user in cycle n.

Computation of the power S_{n+1} is done in accordance to the scheme described in the previous section with consideration of the possible transition paths. The new state probabilities S_{n+1} can be computed from S_n by first determining the corresponding super-state vector $\bar{S}_n$ and multiplying it recursively with the corresponding transition probability matrix $\mathcal{P}_n$ (also known as the power method).

$$\bar{S}_{n+1} = \bar{S}_n \cdot \mathcal{P}_n$$

The transformation from $\bar{S}_{n+1}$ to S_{n+1} yields the new state probabilities. This can be achieved easily by adding all super-states which have a common last state.

$$s_n(j) = \sum_{j_1, j_2} \bar{s}_n(j_1, j_2, j) \qquad j = 0, \ldots, J$$

Since we are interested in the dynamic behavior of the system, we will examine the reaction time until the system converges from one stable condition to another. We will focus in this paper on the impact of the power control algorithm on two important parameters: the number of users currently served within this cell and the distance of the observed user from the base station. The effects of varying these two parameters on the mean mobile transmit power will be studied. It will also be possible to work with higher moments as we obtain the complete power distribution, should this become necessary.

The choice of the initial vector at time $n = 0$ has a great impact on the speed of convergence in the system. To make sure that the system originates from a steady state and is no longer transient, we need to perform a stationary analysis, in which we will derive a power distribution that is independent of the time n. This is an estimation for a steady state distribution that we will also use in our experiments as initial power for the non-stationary experiments.

3.4 Stationary Case

In this section we assume a stationary power control case. Stationary in this sense means that the probability distributions of the random variables S_n are independent of n. We can then drop the index n denoting the power control cycle to obtain $\bar{S} = \lim_{n\to\infty} \bar{S}_n$ and $X = \lim_{n\to\infty} X_n$. Please, note that with $\bar{S}$ we denote the super-states in our system and not our original states representing the power levels.

Solution of this Markov process is straightforward [4]. Since the transition probabilities of these states are given, we can compute the solution of the state probabilities by solving the following homogeneous linear Eqn. (3).

$$\Big(\bar{s}(0,0,0), \ldots, \bar{s}(J,J,J)\Big) \cdot (\mathcal{P} - \mathcal{I}) = \mathcal{O} \tag{3}$$

Here, $\mathcal{I}$ is the identity matrix and $\mathcal{P}$ the transition probability matrix with entries $u(j)$ and $d(j)$.

The resulting distribution of the stationary mobile transmit power located at a distance of 2000 m from the base station in a cell with 15 users is depicted in Fig. 5. As expected the mobile power follows a normal distribution in dB which corresponds to log-normal when transformed into linear space.

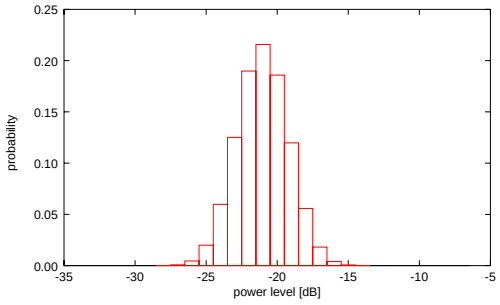

Figure 5: Stationary transmit power distribution

Figure 6 illustrates that the mean stationary mobile transmit power for an observed user increases with the number of users in the cell. The mean approaches the maximum power level and causes the signal to exceed the dynamic range for an increasing distance from the mobile to the base station.

3.5 Probability of Exceeding the Dynamic Range

From our state space description it is easy to obtain an expression for *range exceeding* (RE). This is defined here as the probability that channel and/or interference conditions will require the mobile's transmitter to exceed the maximum permissible power. This occurs in the super-states $(J-1, J, J)$ and (J, J, J) as illustrated in Figure 4.

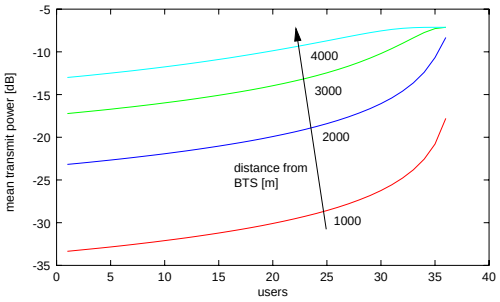

Figure 6: Mean power as function of users

The probability to be in an RE state can then be given as:

$$P_{\mathrm{RE}} = \bar{s}(J-1, J, J) + \bar{s}(J, J, J).$$

Figure 7 shows the corresponding curve for range exceeding as function of the distance of the observed user from the BTS. Let us now define the random variable Y as the

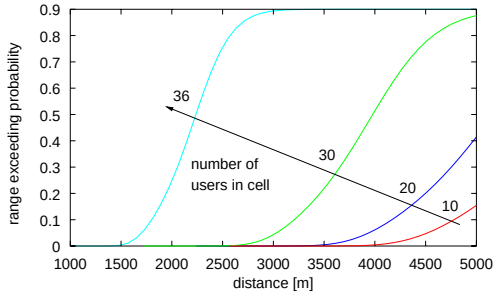

Figure 7: Range exceeding probability as function of distance

number of successive RE cases. We can easily obtain the distribution of Y under the condition that we have an RE as:

$$P(Y = i \mid \mathrm{RE}) = \begin{cases} d_{J-1} & i = 1 \\ u_{J-1} \cdot u_J^{i-1} \cdot d_J & i > 1 \end{cases} \quad (4)$$

In order to get an unconditioned probability for the number of successive range exceeding cases, we need to uncondition Eqn. (4) with P_{RE}.

The probability distribution of Y is illustrated in Fig. 8. In this scenario we assumed the user to be located at a distance of 3000 m from the BTS and varied the number of users in the cell. The probability of exceeding the dynamic

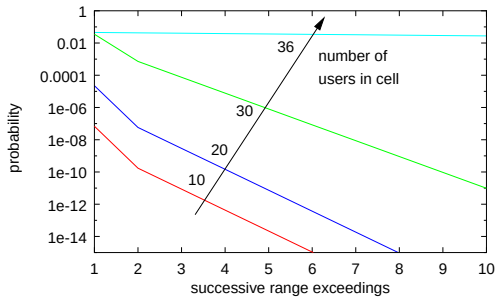

Figure 8: Probability distribution of successive range exceeding events

transmitter range determines the outage probability which in turn influences the *quality of service* (QoS) in a cell and is therefore an important component in network dimensioning and planning [11].

4 RESULTS

To observe the time dependent dynamic behavior of our model we conducted several experiments where we varied the number of users in the system. We assumed an already "perfectly" power controlled system obtained by the stationary analysis with initially $k_0 = 15$ users and added $\Delta k = 5$ users to the system. We measured the power control cycles it took for the system to again reach a stable state and compared the iterative result with the one obtained theoretically from the stationary analysis. Once stability was reached, we removed the Δk users again until we had our initial number of k_0 users. In Fig. 9 the mean power of this experiment is given. Note that the mean power overshoots the target value and converges after oscillating about the theoretical mean. Performing the same experiment for

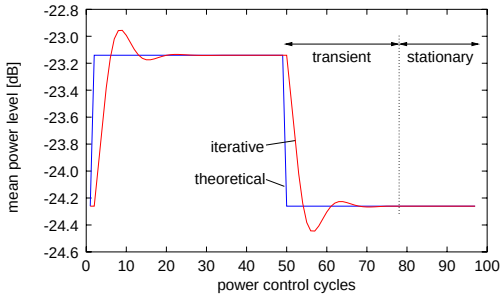

Figure 9: Mean power of non-stationary analysis

different values of k_0 at a fixed observer distance of 1000 meters, we get Fig. 10 for the number of power control cycles until stability is reached when adding users and Fig. 11 for leaving users. Both figures show the sensitivity of the system for bulk arrivals and departures. The staircase shape of the curves stems from the fact that we do not have any fractional power control cycles as this is our smallest unit of time. In Fig. 10 we add to a system already contain-

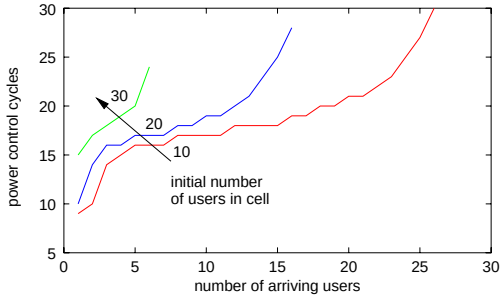

Figure 10: Convergence time for bulk arrivals

ing $k_0 = 10, 20, 30$ users Δk further users until the pole

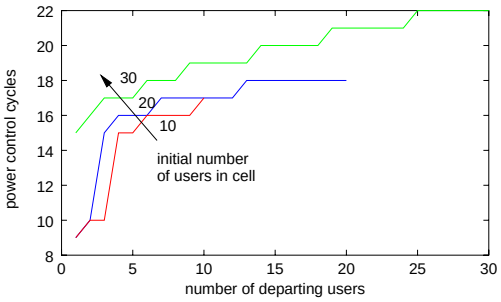

Figure 11: Convergence time for bulk departures

capacity is reached or the range exceeding probability of this state is greater than 10%. It is clear that a system with a higher load requires more time to converge to a stable state. The same effect can be seen when removing Δk customers from the system. Naturally only a maximum of k_0 can be removed. It can be also seen when comparing both figures that the time for removing Δk users is shorter than for adding the same number.

When observing a user that enters the system at a certain distance in a cell that is currently loaded with $k = 10, 20, 30$ users, we obtain Fig. 12. What can be seen is

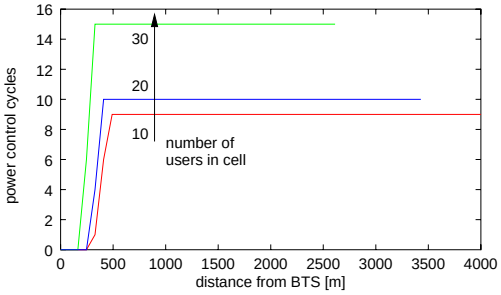

Figure 12: Convergence time over the distance from the BTS

that the higher loaded the cell is, the longer it takes until a stable state is achieved. The most striking fact, however, is that as long as no RE case occurs, the time for convergence is independent of the distance of the new user.

5 CONCLUSION AND OUTLOOK

In this paper we presented a new analytic description of the reverse link power control in an IS-95 CDMA system. We observed that the transmit power for an arbitrary observed mobile user follows a log-normal distribution and is very sensitive to the current level of multi-access interference in the cell. This has an effect on the quality of service in the cell in terms of increased signal range exceeding probability. The variation of the system parameter settings showed that the reaction time for batch arrivals and departures in the cell is also mainly influenced by its current load, but less dependent on the distance-induced propagation loss.

Our approach so far only considered an *additive white Gaussian noise* (AWGN) channel with no time dependent behavior. In reality, however, correlations in the fading channel cause the propagated signal to fluctuate at a greater degree. One of our next aims is therefore to include a model that considers fading in a more realistic manner by modifying the loop driving variable.

The results presented here include the inner loop only (which uses SIR as the performance measure) and do not yet include outer loop processing based on frame-error statistics [9]. Another possible extension of the current model is to include the effects of the open-loop power control which would allow direct computation of the total mobile transmit power statistics. Both of these topics are slated as future work.

ACKNOWLEDGMENT

The authors would like to thank Wolfgang Jodl for his programming efforts as well as Notker Gerlich (University of Würzburg), Nikhil Jain (Qualcomm Inc.), and Mohamed Landolsi (NORTEL Wireless Networks) for the valuable discussions and help during the course of this work. Part of this work has been supported by NORTEL External Research.

References

[1] S. Ariyavisitakul and L. F. Chang. Signal and interference statistics of a CDMA system with feedback power control. *IEEE Transactions on Communications*, 41(11):1626–1634, November 1993.

[2] R. D'Avella, D. Marizza, and L. Moreno. Power control in CDMA systems: Performance evaluation and system design implications. In *Proc. of the IEEE International Conference on Universal Personal Communication*, pages 73–77, San Diego, CA, September 1994.

[3] D. Kim, K. Chang, and S. Kim. Efficient distributed power control for cellular mobile systems. *IEEE Transactions on Vehicular Technology*, 46(2):313–319, May 1997.

[4] L. Kleinrock. *Queueing Systems*, volume 1. John Wiley & Sons, 1975.

[5] D. Mitra and J. A. Morrison. A novel distributed power control algorithm for classes of service in cellular CDMA networks. In *Proc. of the Sixth WINLAB Workshop on Third Generation Wireless Information Systems*, pages 141–157, New Brunswick, NJ, March 1997.

[6] R. Padovani, B. Butler, and R. Boesel. CDMA digital cellular: Field trial results. In *Proc. 44th IEEE Veh. Tech. Conf.*, pages 11–15, Stockholm, Sweden, June 1994.

[7] R. Pincha, Q. Wang, and V. K. Bhargava. Non-ideal power control in DS-CDMA cellular. In *Proc. of the IEEE Pacific Rim Conference on Communications*, pages 686–689, 1993.

[8] T. S. Rappaport. *Wireless Communications – Principles & Practice*. Prentice Hall, Upper Saddle River, NJ, 1996.

[9] A. Sampath, P. Sarath Kumar, and J. M. Holtzman. On setting reverse link target SIR in a CDMA system. In *Proc. of the IEEE 47th Veh. Tech. Conf.*, pages 929–932, Phoenix, AZ, May 1997.

[10] TIA/EIA/IS-95. Mobile station – base station compatability standard for dual–mode wideband spread spectrum cellular systems. Technical report, Telecommunications Industry Association, July 1995.

[11] P. Tran-Gia, K. Leibnitz, and N. Jain. Code division multiple access wireless network planning considering clustered spatial customer traffic. In *Proc. 8th International Telecommunication Network Planning Symposium*, Sorrento, Italy, October 1998.

[12] A. J. Viterbi. *CDMA - Principles of Spread Spectrum Communication*. Wireless Communications Series. Addison-Wesley, 1995.

[13] A. J. Viterbi, A. M. Viterbi, and E. Zehavi. Performance of power–controlled wideband terrestrial digital communication. *IEEE Transactions on Communications*, 41(4):559–569, April 1993.